

## Multivariate Standard Normal Transform: Advances and Case Studies

Ryan M. Barnett and Clayton V. Deutsch

*The Multivariate Standard Normal Transformation (MSNT) was recently proposed to transform arbitrary multivariate data to a standard normal distribution. The MSNT was constructed as an optimization problem, where complex multivariate data are mapped directly to a multivariate Gaussian distribution in a manner that minimized changes to the original multivariate structure. While the original idea is carried forward, conceptual and algorithmic details have been significantly altered. The MSNT concept will first be redeveloped, followed by an overview of its implementation. Case studies are presented to demonstrate the MSNT on data of various forms. While promising results are shown, work remains for the MSNT to be applicable on data sets composed of many observations.*

### Introduction

Out of practical necessity, the multivariate Gaussian distribution is commonly adopted within geostatistics for modeling spatially correlated random variables. As geologic variables are often non-Gaussian in nature, a wide variety of techniques [2] are available to transform them to a multiGaussian form, with their associated back-transforms to reintroduce the original distributions. The well-known and widely applied normal score transformation [2,4] will guarantee univariate Gaussianity, however, multivariate Gaussianity is rarely achieved by this transform. The stepwise conditional transform [12] is the most commonly used transform which attempts to make the data multivariate normal. While very useful when working with 2 or 3 variables and over 1000 data, the binning nature of stepwise prevents its natural application on larger dimensional datasets. Other less common transforms exist that will not be enumerated [1,2,13], though they may be summarized as having similar deficiencies related to dimensional restrictions. A very large problem which remains in the geostatistical field is a transform that: (i) transforms geologic data to be perfectly multivariate Gaussian, (ii) fully captures on the forward transform (and reintroduces on the back-transform) all of the original univariate and multivariate complexities, and (iii) is applicable to any realistic dimension of geologic data (2-100 variables).

Originally proposed in a paper of the same title, the Multivariate Standard Normal Transformation (MSNT) [4] has the potential to possess all of the ideal multivariate Gaussian transform qualities that are outlined above. At the time of its original release, the MSNT was in its infancy of development and required further research into implementation details. The following paper will present the latest version of the MSNT. To avoid comparing the numerous changes that have been made from its original form, the MSNT concept will be redeveloped before outlining the major points of its current implementation. This will include periodic discussion on alternative approaches that could be considered at various steps of the algorithm, which may have been rejected based on prior testing, or represent future research directions. A 2-D synthetic dataset is used for demonstration during this algorithm outline due to its visual simplicity. The MSNT is then applied to a 3-D Nickel Laterite dataset of greater non-linear and stoichiometric complexity as a final realistic geometallurgical case study.

### MSNT Concept, Transform Distortion, and Visualization

As the MSNT is composed of several steps, it may be easy to lose sight of the overarching concept when proceeding through the details that are outlined in the next section. To avoid this, the MSNT concept, objectives, and end results are immediately presented in this section. Additionally, methods that will be used later for judging the transform's results will be discussed.

The MSNT transforms a complex  $k$ -variate distribution of  $N$  observations, to a  $k$ -variate Gaussian distribution of  $N$  observations. This is achieved by directly mapping observations between the two distributions using a single index vector  $M$  of length  $N$ . The concept may be more easily understood according to the schematic illustration in Figure 1, where arrows represent the indexed mapping. Although this is a remarkably simple concept, the question arises of what criteria should be sought after when attempting to map between the distributions? What defines a good mapping?

It is proposed, that a good mapping will minimize the distortion of the original data configuration when transforming the data to Gaussian space. Distortion is defined here based on the relative configuration of the data. Neighboring observations in original space should remain near to one another in transformed space. Likewise, widely separated observations in original space should remain distant in transformed space. According to this definition, the absolute location or magnitude of a data observation in original and transformed space is not considered of primary importance. Rather, distortion is a function of changes that occur to the distances between observations. A good Gaussian mapping transform should minimize these changes. With this in mind, the MSNT is posed as an optimization problem, with an objective function that seeks to minimize the changes that occur to the distances between observations in original and transformed space.

With the success of a Gaussian mapping now defined based on the relative shift that occurs between observations, a method will be required for visualizing the results and judging the success of the transform. As the mapping arrows in Figure 1 already begin to create clutter, it is easy to imagine that they will only add confusion when plotting realistic datasets of >100 observations. Perhaps the most effective method for judging results, is through coloring the transformed observations according to their associated values in original space. To illustrate this idea, both distributions and the mapping arrows in Figure 1 are colored according to the Z1 value. While it was specified above that maintaining the absolute magnitude of an observation in original space is not critical to the success of the transform, it remains an effective way for judging how the position of observations have shifted relative to one another. Ideally, we wish to see a continuous gradient of color in transformed space, since this indicates that the mapped observations originated from similar locations as measured in one dimension. Coloring according to multiple dimensions may then take place. Note that as the dimension coloring in the transformed distribution of Figure 1 is quite chaotic, this would represent a poor mapping.

As will be demonstrated, distortion will also manifest itself in the variograms of the transformed variables. While the variograms of transformed variables are expected to change relative to their original form, a high degree of distortion will destroy any meaningful spatial structure. Throughout the remainder of this paper, the success of the MSNT will be based on this dimension coloring concept and inspection of the transformed variograms.

### MSNT Steps

The following section will outline the major steps of the MSNT, using a 2-D synthetic dataset for demonstration. This data is displayed in Figure 2, where complex multivariate features such as heteroscedsticity and mild non-linearity are observed between the variables. Note also that the two variables possess varying spatial structure according to their experimental variograms.

#### *Step 1: Normal score transform the data to obtain the Original Distribution*

As subsequent mapping steps will revolve around the euclidean distance between observations, the MSNT will be very sensitive to drastically different units or outlier values. The widely-applied normal score transform [2,5] standardizes variables to the same units<sup>1</sup> and removes outlier values to resolve both issues. The normal score transform is given by Equation 1, where quantile matching is performed between the empirical data CDF,  $F$ , and the standard normal CDF,  $G$ . This step is demonstrated on the 2-D synthetic data in Figure 3, where marginal histograms are observed in the transformed  $y$  data. While potentially confusing, it is  $y$  (rather than  $z$ ) that has been (and will be) referred to as the original distribution. This is because  $y$  will be the origin of the subsequent mapping.

$$y = G^{-1}(F(z)), \quad F(z) \in [0,1] \quad (1)$$

#### *Step 2: Generate the Transformed Distribution using LHSMDU*

With the origin of the MSNT mapping in a suitable form according to Equation 2, a multivariate Gaussian distribution  $g$  must now be generated as the destination of the mapping. This transformed distribution  $g$  will be  $N$  observations and  $k$  dimensions in accordance with the original  $y$  distribution. This step is

---

<sup>1</sup> In addition, these units attractively coincide with the units of the transformed distribution  $g$ .

represented by Equation 2, where  $F(z)$  are randomly generated CDF values, used to attain Gaussian values according to the empirical standard normal CDF,  $G$ .

$$g = G^{-1} \left( \begin{bmatrix} F(z)_{11} & \dots & F(z)_{1N} \\ \vdots & \ddots & \vdots \\ F(z)_{k1} & \dots & F(z)_{kN} \end{bmatrix} \right), F(z)_{ij} \in [0,1] \quad (2)$$

Monte Carlo simulation (MCS) [6] could be considered for generating the random  $F(z)$  values, but as demonstrated in Figure 4, it produces unsatisfactory multivariate Gaussian distributions due to non-uniform sampling. Latin hypercube sampling with multidimensional uniformity (LHSMU) [6] is adopted as a result to insure multivariate uniformity of the  $F(z)$  values. Uncorrelated and correlated multivariate Gaussian distributions generated by the LHSMU are displayed in Figure 4. The correlated distribution is constructed according to the correlation of the 2-D  $y$  data from Figure 3, and will be treated as the  $g$  transformed distribution for the synthetic case study in subsequent steps. An even higher degree of Gaussianity could potentially be achieved using methods such as Gauss-Hermite quadratures [9], which may be applied in the future.

While it is clear that  $g$  should be as multiGaussian as possible, the decision on whether this transformed distribution should be correlated or not may depend on the subsequent modeling framework. For example, if independent simulation is to be executed on the transformed variables, then an uncorrelated distribution may<sup>2</sup> be generated. Conversely, a correlated distribution will be required for dependent simulation methods such as co-simulation.

It is worth noting that this decision may have considerable implications on the transform distortion of the ultimate mapping. Particularly when the original distribution is highly correlated<sup>3</sup>, it makes intuitive sense that distortion should be more easily minimized when mapping distributions of the same correlation. Identically correlated distributions are decidedly more similar in form than correlated and uncorrelated distributions.

### Step 3: Initial Mapping through Dimension Reduction

The original marginally normal distribution  $y$  and the transformed multivariate normal distribution  $g$  have been generated according to the steps above. The initial mapping index vector  $M$  must now be established between them. It is this mapping vector that will be heuristically optimized in the next step and section. A good initial mapping will be necessary for the subsequent optimization to properly converge.

This initial mapping is a dimension reduction problem, as observations of the multidimensional original and transformed distributions must be described by a single measurement that allows for their alignment. Ideally, this single measurement will describe the greatest possible amount of variability in the multivariate data. Once the distributions are measured along this single dimension, they may be sorted and have their initial mapping established accordingly.

This dimension reduction is currently achieved using the classic technique of principal component analysis (PCA) [2,8,10]<sup>4</sup>, which will yield a vector that describes the greatest linear variability in the multivariate data. The first principal component vector  $p$  is the first row of the sorted eigenvector

<sup>2</sup> Even if independent simulation is the eventual goal, a correlated Gaussian mapping may be considered since decorrelation methods such as PCA [2,8,10] or MAF [2,17] could be subsequently applied to the transformed variables. While not appropriate for complex distributions [2], these linear decorrelation methods are very effectively and appropriately applied to correlated multiGaussian data.

<sup>3</sup> Or in the case of greater than 2 dimensions, a highly non-orthogonal correlation matrix.

<sup>4</sup> As the original distribution may be non-linear, a potential improvement with this step could involve the use of non-linear dimension reduction methods. Many such techniques have been tested, including non-linear PCA with auto-associative neural networks [16], kernel PCA [15], and variance unfolding [11]. As compared to linear PCA, results with these non-linear schemes represented significantly worse to very marginal improvements in the resultant mapping. They were consequently not adopted, though many additional techniques remain to be tested.

matrix  $P$ , which is found through the spectral decomposition of the covariance matrix  $C = PDP^T$ . Here,  $C$  is the covariance matrix of the original distribution  $y$ , and  $D$  is the associated diagonal eigenvalue matrix. This is demonstrated on the synthetic data in Figure 5, where the first and second principal component vectors are displayed. It is the larger of these two vectors that is the first principal component vector  $p$ . Both the original distribution  $y$  and transformed distribution  $g$  may be rotated and described along this vector  $p$  according to their respective linear transformations in Equation 3.

$$x = py, \quad x = pg \quad (3)$$

Both multivariate distributions are now reduced to a single variable  $x$  that describes the greatest amount of linear variability in the multivariate distribution  $y$ . Finally, rank order the  $y$  and  $g$  distributions according to their associated  $x$  values to create the initial mapping vector  $M$ .

#### Step 4: Simulated Annealing to Minimize Transform Distortion

The above steps have respectively formed the original distribution  $y$ , the transformed distribution  $g$ , and an initial mapping index vector  $M$  that connects them. Recall that the MSNT seeks to reduce transform distortion, by minimizing the changes that occur to the euclidean<sup>5</sup> distances between observations in original and transformed space. With this in mind, the MSNT objective function is given by Equation 4. Given a specified mapping index vector  $M$ ,  $d_{o(ij)}$  is the distance between the  $i^{\text{th}}$  and  $j^{\text{th}}$  observations in original space, and  $d_{t(ij)}$  is distance between those same observations in transformed space. The decision to make this a quadratic function was based on testing a range of other powers.

$$\min \left[ O = \sum_{i=1}^N \sum_{j=1}^N (d_{t(ij)}^2 - d_{o(ij)}^2)^2 \right] \quad (4)$$

Unfortunately, Equation 4 may not be solved using global linear<sup>6</sup> or convex solvers. Instead, it is accomplished through randomly perturbing the mapping index vector  $M$  in a pairwise fashion using a simulated annealing framework [3]. Ideally, the second summation in Equation 4 will proceed to the full  $N$  number of observations, so that the distances between all observations are considered. While it is important that neighboring observations remain close together, it is equally important that distant observations remain far apart.

As convergence times when considering all observations in this manner can grow prohibitively long for larger datasets (Figure 6),  $N$  may be modified on this second summation to be based on only the nearest  $n$  number of nearest neighbours to the  $i^{\text{th}}$  observation in original space. This is represented by the schematic in Figure 7, where a mapping is made based on the distance between an arbitrary observation and its four nearest neighbours. This indirectly achieves a similar end goal, though inferior results were observed and it is only recommended when using the full  $N$  number of observations is not computationally feasible.

Following this optimization, the resultant index vector  $M$  may (or may not) be considered an acceptable Gaussian mapping transform. To inspect the MSNT results, we return to the concepts of dimension coloring and variogram structure for inferring transform distortion. Dimension color plots and experimental variograms are displayed in Figure 8 for the 2-D data. The initial PCA mapping is also displayed in this figure for reference of what would be considered unacceptable distortion. Variograms of the normal score  $y$  data are provided as a reference of the spatial structure prior to mapping. A large improvement is seen in the distortion of the optimized mapping when compared to the initial PCA

<sup>5</sup> Other distance measures may be considered for highly non-linear data, such as shortest graph distances [7] where graph connections are made between neighbouring observations.

<sup>6</sup> If this mapping is modified to be accomplished in multiple stages, it can become a linear transportation optimization problem that is globally solved using the Hungarian algorithm [14]. Inferior results were found so far with this approach, however, due to the necessity of multiple stages.

mapping. A much smoother gradient of color is observed in the dimension coloring plot, as well as variograms of greater continuity. This illustrates that when the distortion is not minimized, less spatial continuity is preserved. The optimized mapping vector  $M$  is deemed to be an acceptable transform based on these plots.

#### *Backward Transform*

Following any arbitrary modeling methods in Gaussian space, a simulated realization will need to be back-transformed to the original data units. This process for the MSNT will be highly analogous to the univariate normal score transform. Like the normal score transform, the MSNT records the original and transformed value for each observation during the forward transform process. This recorded file simply needs to be referenced for mapping Gaussian values back to original space.

Since the simulated grid nodes will not possess identical values to the mapped observations, an interpolation method is used to infer their location in original space based on their proximity to the nearest mapped observations in Gaussian space. This concept is represented by Equation 5 and displayed schematically in Figure 9, where the  $i^{\text{th}}$  simulated location is back-transformed based on its euclidean distance in transformed space  $d_{i(ij)}$ , to the  $j^{\text{th}}$  mapped observation. This amounts to inverse distance weighting, where  $d_{i(ij)}$  will determine the weight attributed to the original values of the  $j^{\text{th}}$  mapped observation on the  $y_i$  estimate. Any number of nearest mapped observations could be used for this interpolation, but it is advocated that this should be chosen based on the  $k$  number of multivariate dimensions, where  $k+1$  number of observations is optimal. Using less than this does not adequately constrain the multivariate interpolation, but increasing beyond  $k+1$  will begin to converge the back-transformed results towards the mean.

$$y_i = \sum_{j=1}^{k+1} \lambda_j y_j, \text{ where } \lambda_j = \frac{1}{d_{i(ij)}} \text{ and } \sum_{j=1}^{k+1} \lambda_j = 1 \quad (5)$$

Returning to the MSNT transformed synthetic data from Figure 8, MAF [17] will first be used to decorrelate the distribution before independently simulating the variables using SGSIM. The simulated Gaussian variables are then back-transformed through MAF, Equation 5, and the normal score back-transform. Selected model validation plots of the back-transformed Z1 and Z2 realizations are shown in Figure 10, where good reproduction of the univariate, multivariate, and spatial statistics is observed. As it is difficult to gain a sense of whether the joint density of the data is being reproduced by the realizations based on the scatterplots, bivariate Gaussian kernel density estimation (KDE) plots are displayed in Figure 11. Excellent reproduction of the joint density is observed according to this figure.

#### **Case Study**

Nickel laterite data composed of 933 observations and 3 variables (Ni, Fe, and SiO<sub>2</sub>) will be used to demonstrate a geostatistical MSNT based modeling framework. As observed in the scatterplots of Figure 12, complex multivariate features are present including non-linearity, and stoichiometric constraints. Since the variables are compositional, the workflow uses a logratio transform [2]. This is followed by the normal score transform and MSNT mapping to attain a correlated Gaussian transform.

Based on dimension coloring and variography in Figure 13, the MSNT has transformed the data with considerably more distortion relative to that which was seen in the synthetic case study. This is reflected in the large loss of spatial structure that is observed in the transformed variograms, relative to the original normal score variograms. This volume of distortion would suggest that the MSNT is unsuited for this data, as the larger number of observations is preventing the combinatorial optimization from properly converging to a reasonable local minima. Based on testing, this is an issue attributed to observations rather dimensions, as the MSNT has completely very successfully on 6-variate data of lesser observations.

This case study will be carried forward in spite of these large concerns, to demonstrate the type of issues that will result from a poor mapping. After decorrelating the transformed distribution with MAF, SGSIM is then used to independently simulate the uncorrelated Gaussian variables. Back-transforms are

then applied to return the realizations to original space. Validation plots are displayed in Figures 14 and 15, where reasonable reproduction of the multivariate structure is observed based on bivariate scatterplots and KDE plots. Of great concern, however, is the poor reproduction of spatial correlation and marginal histograms in the realizations. This was to be expected based on the large transform distortion that was observed, particularly in the case of the variogram reproduction. These issues are also partially attributed to stationarity concerns unrelated to the MSNT.

### Conclusions

The MSNT is an exciting new data transform that has a wide range of potential applications in its current form. While the MSNT has made large advances from its original implementation and results, its aspirations as a multivariate transform that is applicable to data sets of any size and dimension has not yet been achieved. Many potential branches of future research into the method exist as briefly outlined. The primary concern that remains to be addressed, however, is its sensitivity to large data sets. Both its execution speed and end results significantly degrade with increasing observations as demonstrated. It is not yet clear whether this can be effectively resolved.

### References

- 1 Barnett, R. (2011). Conditional Standardization: A multivariate transformation for the removal of non-linear and heteroscedastic features. *CCG Annual Report 13*, Paper 310.
- 2 Barnett, R. (2011). *Guidebook on Multivariate Geostatistical Tools*. Edmonton, Alberta: Centre for Computational Geostatistics.
- 3 Deutsch, C. (1992). *Annealing techniques applied to reservoir modeling and the integration of geological and engineering (well test) data*. PhD Thesis, Stanford University, California, USA.
- 4 Deutsch, C. (2011). Multivariate Standard Normal Transformation. *CCG Annual Report*, Paper 101.
- 5 Deutsch, C., & Journel, A. (1998). *GSLIB: A geostatistical software library and user's guide, second edition*. Oxford University Press.
- 6 Deutsch, J., & Deutsch, C. (2012). Latin hypercube sampling with multidimensional uniformity. *Journal of Statistical Planning*, vol.142, pp.763-773.
- 7 Dijkstra, E. (1959). A note on two problems in connexion with graphs. *Numerische Mathematik*, pp.269-271.
- 8 Hotelling, H. (1933). Analysis of a complex of statistical variables into principal components. *Journal of Educational Psychology*, 24, 417-441.
- 9 Jackel, P. (2005, May 16). *A note on multivariate Gauss-Hermite quadrature*. Retrieved August 23, 2012, from Selected Documents of Peter Jackel: <http://www.pjaeckel.webspace.virginmedia.com/ANoteOnMultivariateGaussHermiteQuadrature.pdf>
- 10 Johnson, R., & Wichern, D. (1988). *Applied Multivariate Statistical Analysis*. New Jersey: Prentice Hall.
- 11 Kruger, U., Zhang, J., & Xie, L. (2007). Developments and Applications of Nonlinear Principal Component Analysis - a Review. In *Principal Manifolds for Data Visualization and Dimension Reduction* (pp. 1-43). Lecture Notes in Computational Science and Engineering, Volume 58: Springerlink.
- 12 Leuangthong, O., & Deutsch, C. (2003). Stepwise conditional transformation for simulation of multiple variables. *Mathematical Geology*, vol.35, no.2, pp.155-173.
- 13 Manchuk, J., & Deutsch, C. (2011). A program for data transformations and kernel density estimations. *CCG Annual Report 13*, Paper 116.
- 14 Munkres, J. (1957). Algorithms for the Assignment and Transportation Problems. *Journal of the Society for Industrial and Applied Mathematics*, vol.5, pp.32-38.
- 15 Schoelkopf, B., Smola, A., & Mueller, K. (1999). Kernel principal component analysis. *NIPS*, 12.
- 16 Scholz, M., & Vigarito, R. (2002). Nonlinear PCA: a new hierarchical approach. Verleysen, M.(ed.) *Proceedings ESANN*. pp439-444.
- 17 Switzer, P., & Green, A. (1984). Min/Max autocorrelation factors for multivariate spatial imaging. *Stanford University: Department of Statistics Technical Report No.6*, pp.14.

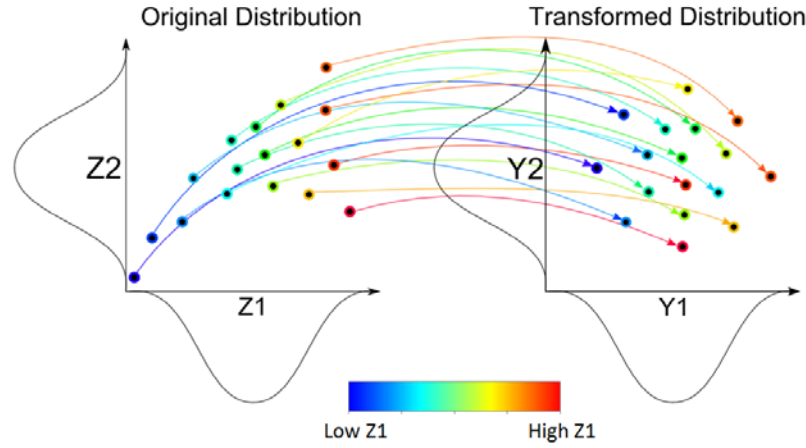


**Figure 1:** Conceptual schematic of MSNT mapping from a complex multivariate distribution (original) and a multivariate Gaussian distribution (transformed).

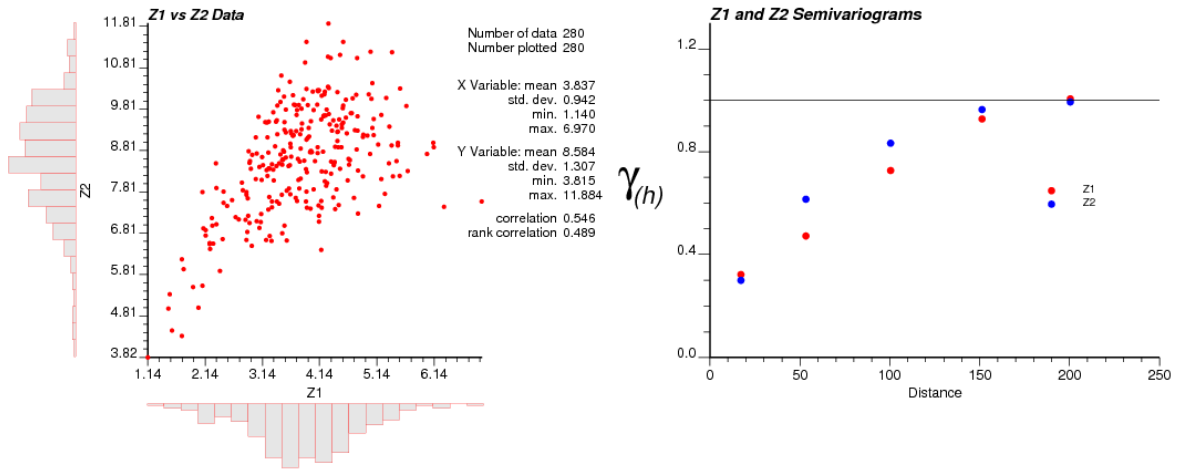


**Figure 2:** Scatterplots, histograms, summary statistics and experimental semivariograms of the 2-D synthetic data.

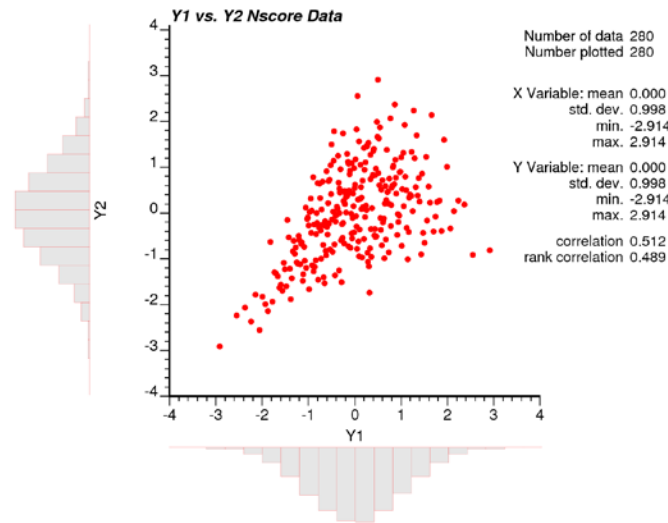


**Figure 3:** Scatterplots, histograms, and summary statistics of the normal score 2-D data.

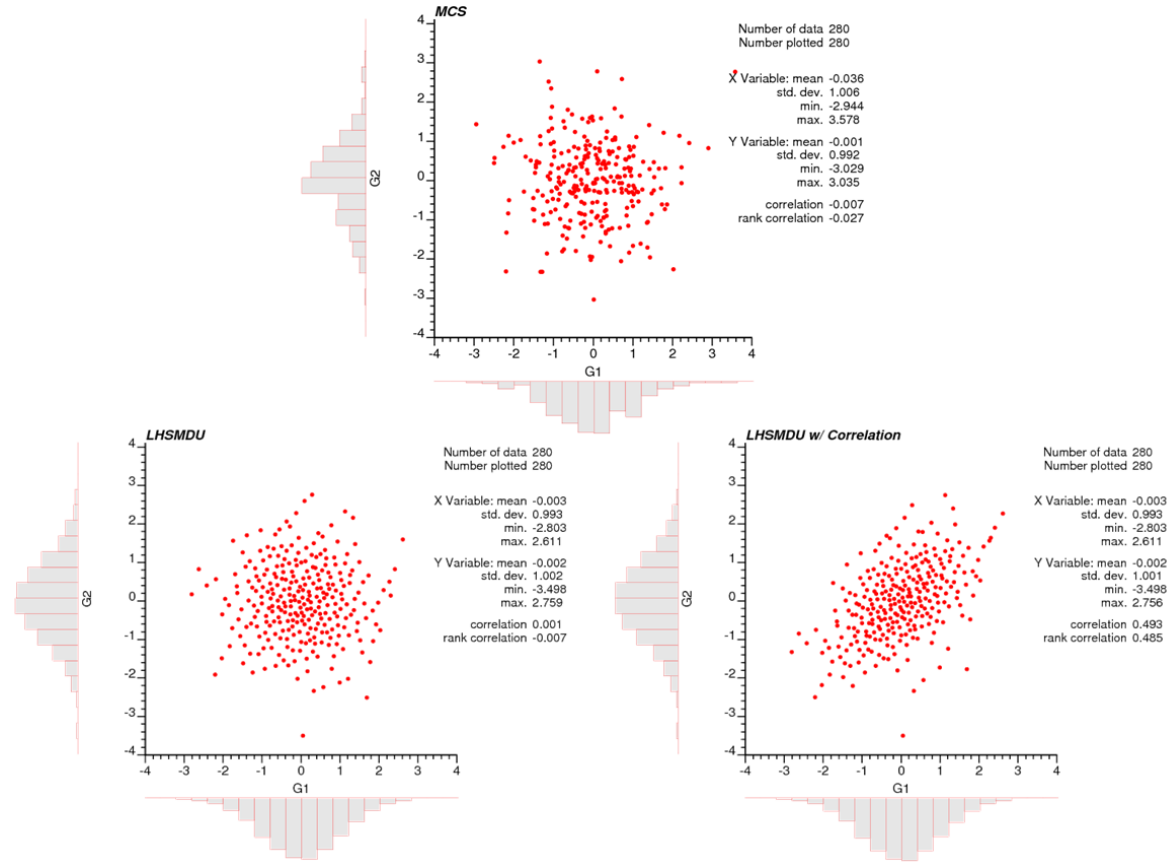


**Figure 4:** Scatterplots, histograms, and summary statistics for two random variables using MCS (left), LHSMDU without correlation (middle), and LHSMDU with correlation (right).

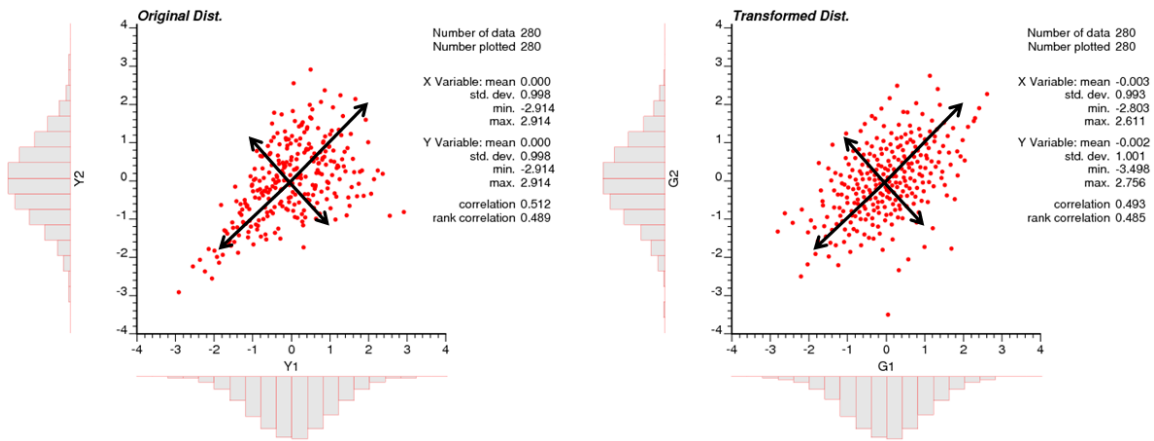


**Figure 5:** Scatterplots of the original and transformed distribution for the 2-D synthetic data with their two principal component vectors overlain.



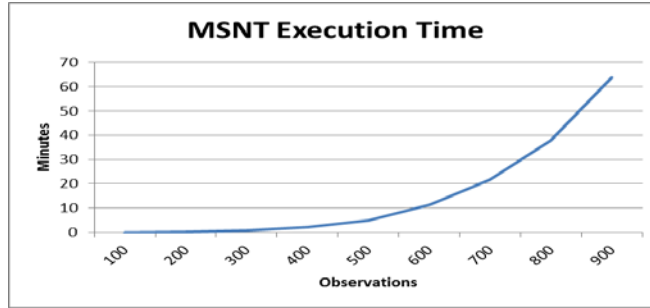


Figure 6: MSNT execution time based on a changing number of observations.

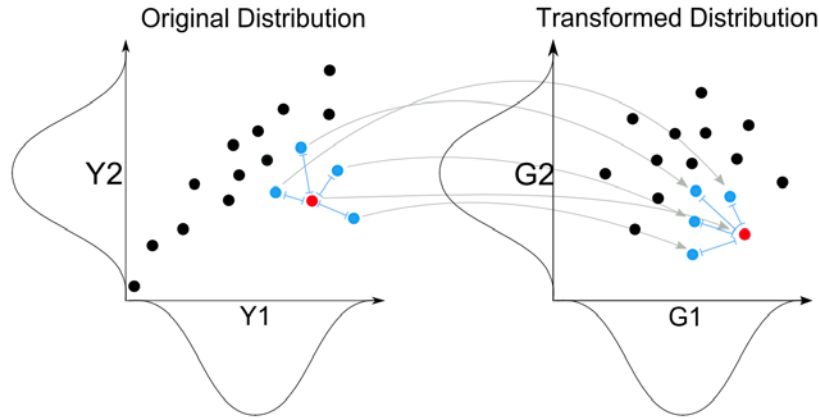


Figure 7: Schematic representation of the original ( $d_{o(ij)}$ ) and transformed ( $d_{t(ij)}$ ) distances between the  $i^{th}$  mapped observation and its four nearest neighbours.

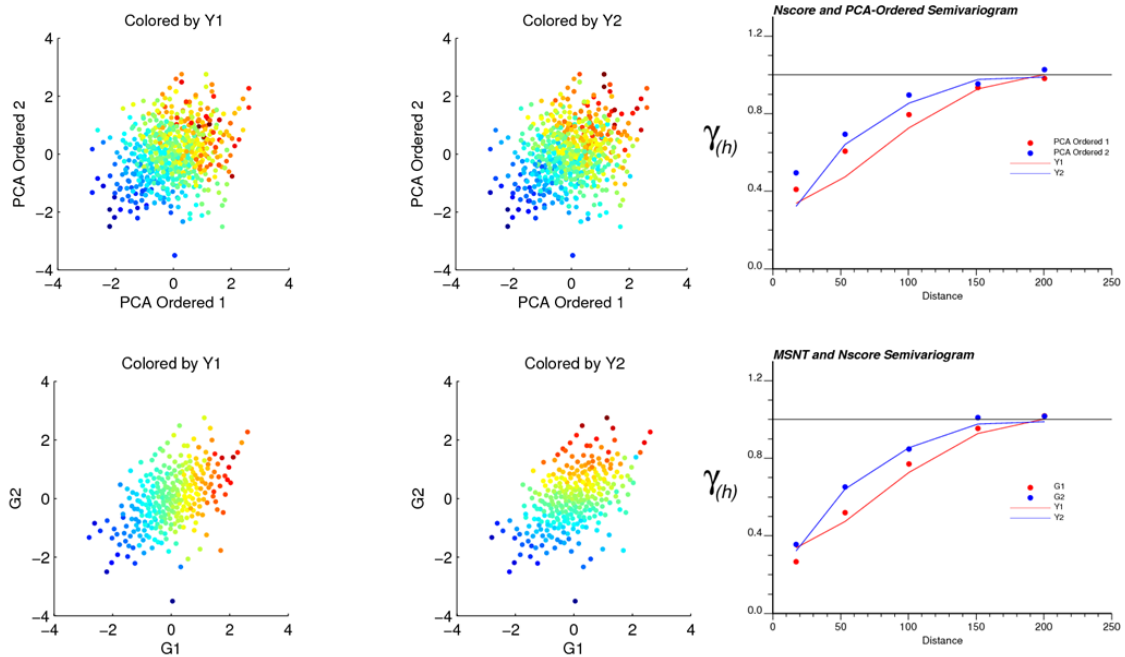
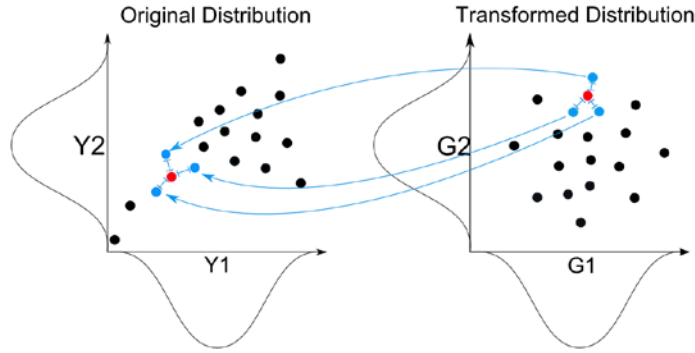
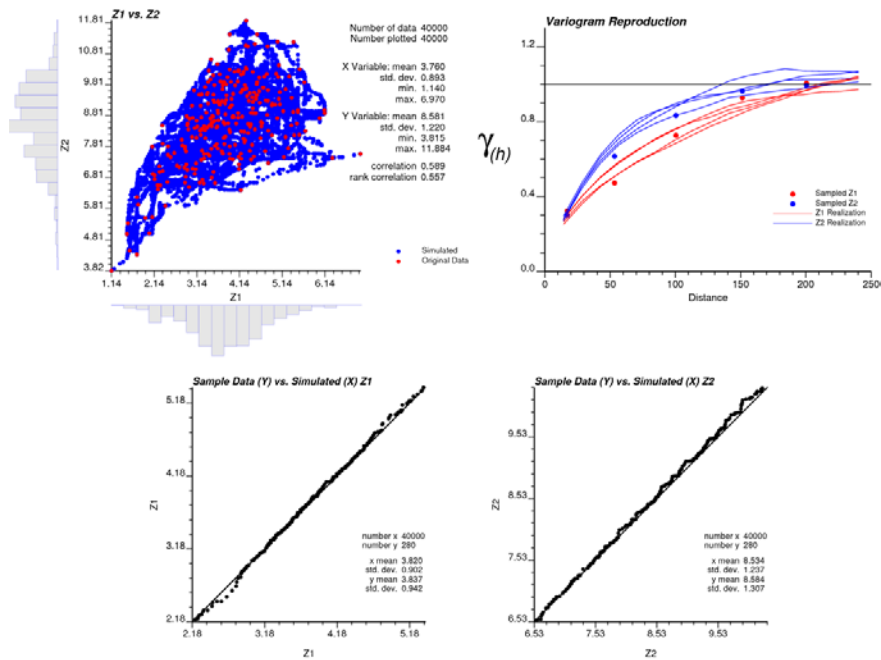


Figure 8: Dimension colored scatterplots and experimental semivariograms of the transformed data following PCA ordering (top) and the full MSNT transform (bottom). The experimental semivariograms of the normal score Y variables is provided for reference of the spatial structure before transformation.



**Figure 9:** Schematic figure of the MSNT back-transformation, where a simulated location is back-transformed based on its proximity to the nearest 3 mapped observations.



**Figure 10:** Selection of model validation plots. Scatterplot of the original data overlain on four back-transformed realizations, with marginal histograms and summary statistics of the realizations (top left). Experimental semi-variograms of the original data and the four realizations (top right). Q-Q plots between the realizations and the original declustered data (bottom).

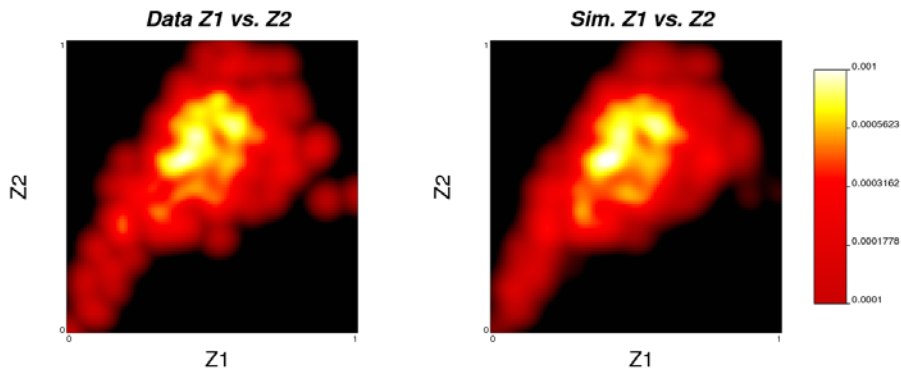


**Figure 11:** Gridded bivariate Gaussian KDE of the original data (left) and simulated realization (right).

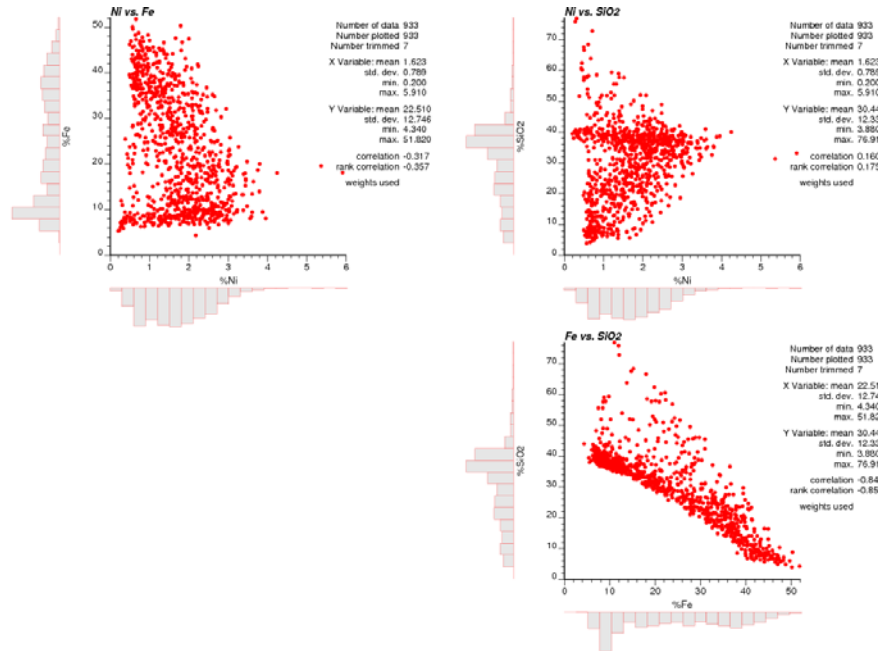


Figure 12: Scatterplots between Ni, Fe, and SiO2 for the Nickel laterite data.

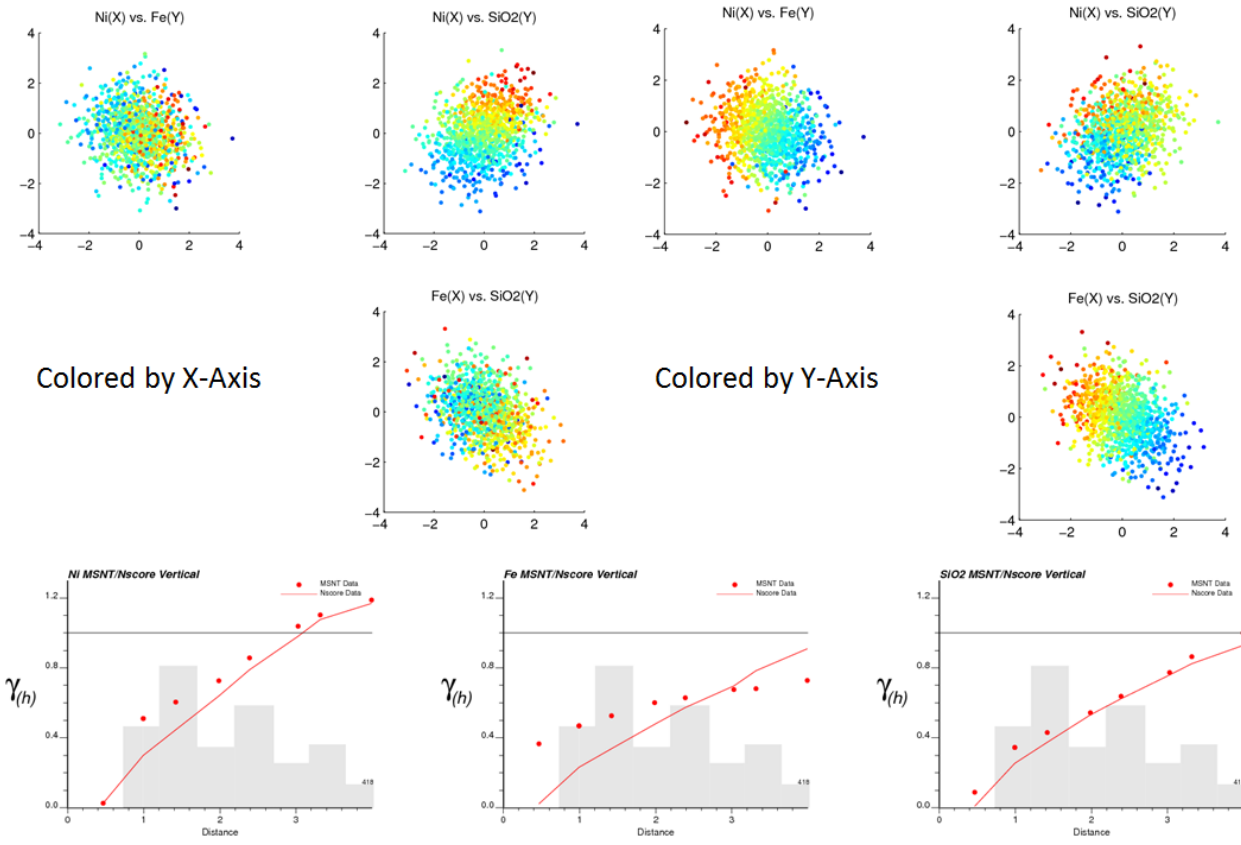
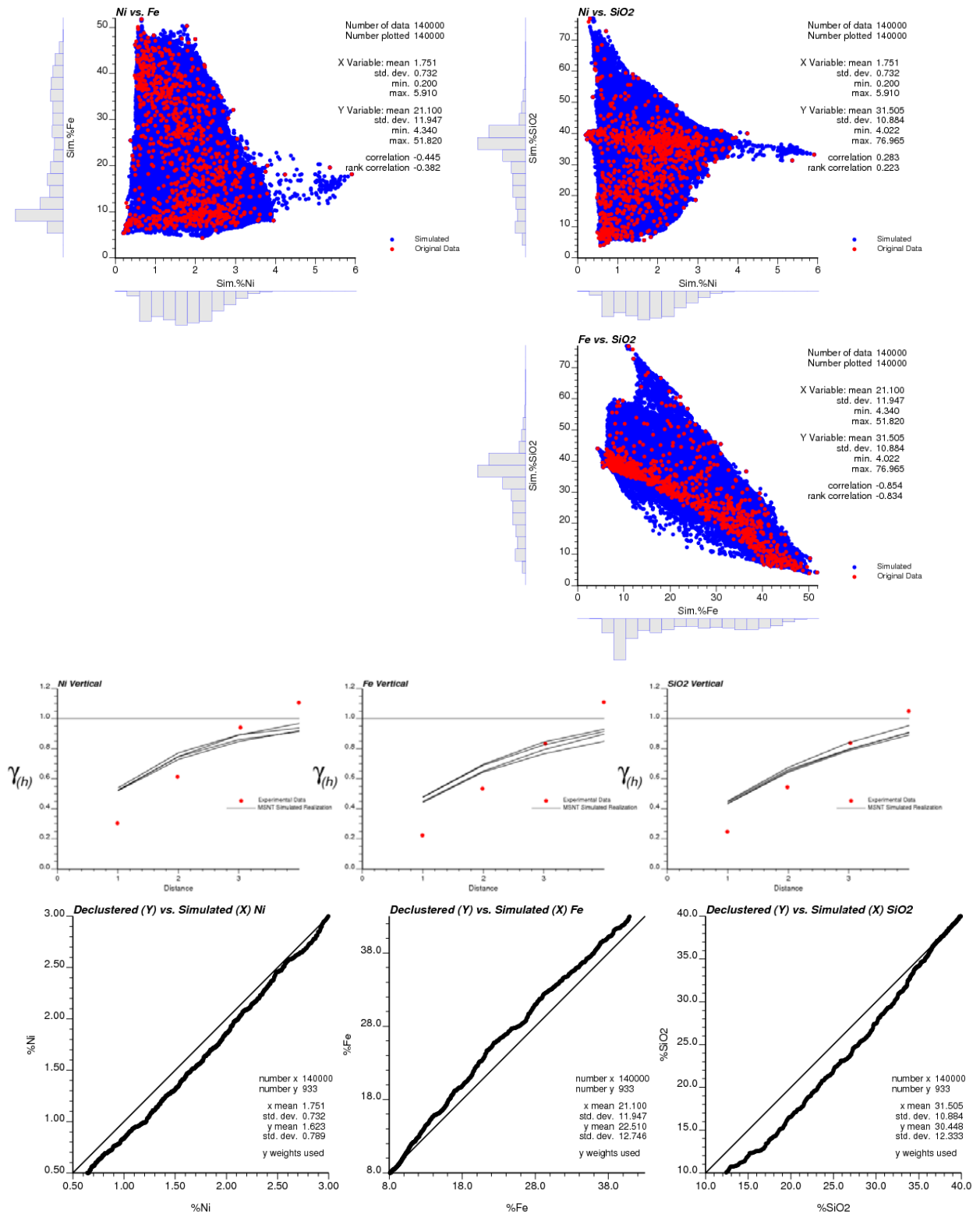
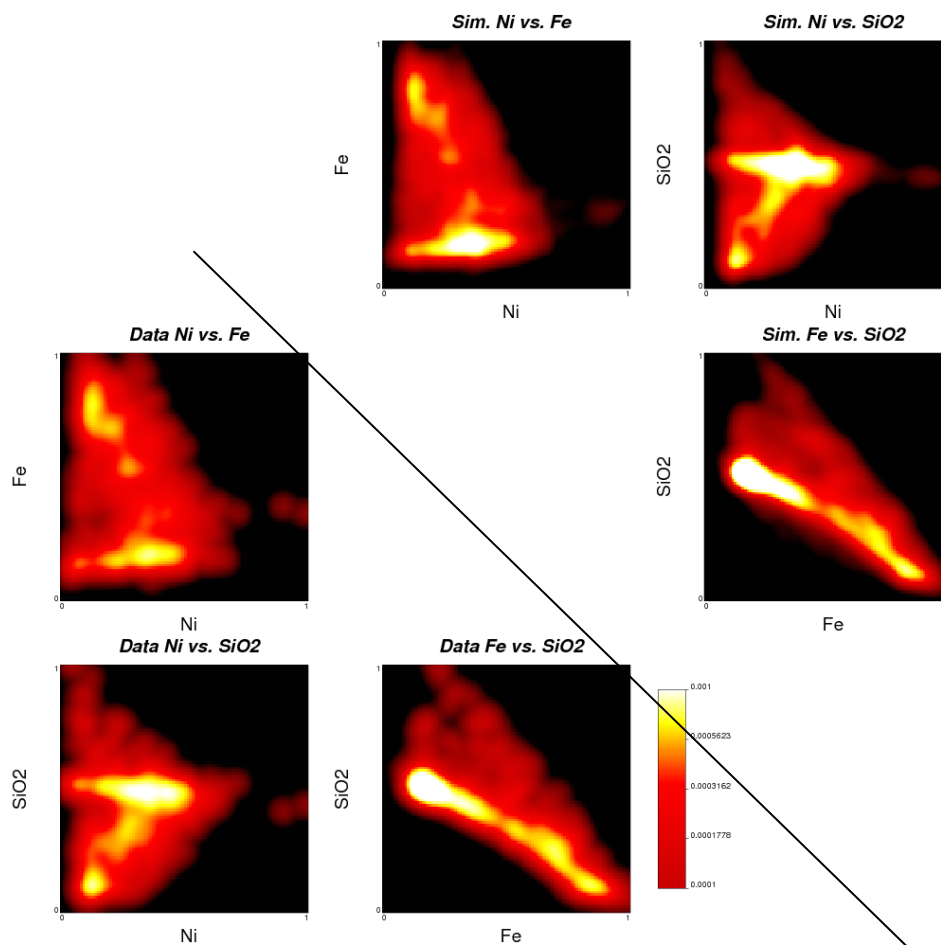


Figure 13: Scatterplots between the transformed Nickel laterite variables, where each point is colored by the Y value of its respective x-axis variable. The experimental semivariogram before (line) and after (dots) transformation are shown on the bottom. The relative number of pairs used in the calculation of each variogram is given by the grey histogram.



**Figure 14:** Selection of model validation plots. Scatterplot of the original data overlain on four back-transformed realizations, with marginal histograms and summary statistics of the realizations (top). Experimental semi-variograms of the original data and the four variables (middle). Q-Q plots between the realizations and the original declustered data (bottom).



**Figure 15:** Gridded bivariate Gaussian KDE of the original data (bottom covariance matrix triangle) and four back-transformed realizations (upper covariance matrix triangle).

## Appendix

Parameters for the FORTRAN coded standalone executable `msnt` (MSNT forward transform) are displayed in Figure 14 and described below:

- **datafl:** file with the data to be transformed (must be normal score transformed as values beyond  $|5|$  are trimmed automatically).
- **nvar:** number of variables to be transformed.
- **icol(i), i=1,...,nvar:** column locations in the **datafl** where the original values of the variables are located.
- **nclose:** number of nearest observations that should be considered when optimizing. Setting this value to **0** will cause the distances between all observations to be considered. This has large speed implications, but will produce the best results if time allows.
- **ixv(1):** random number seed used to determine the starting location of the Gibbs sequence
- **icorr:** if set to **1**, the normal score correlation matrix of the original data will be used for generating a correlated transformed distribution. If set to **0**, the generated transformed distribution will be uncorrelated.

- **outfl**: output file containing input data with the transformed variables appended. This output data file may also be referenced as a transform table for back-transforming simulated results.

```

1      Multivariate Standard Normal Transformation
2      *****
3
4  START OF PARAMETERS:
5  data.dat      -data file
6  2             -nuber of variables
7  1 2          -column numbers
8  0            -number of close values (0=all)
9  69069        -random number seed
10 1            -use nscore correlation?(0=no,1=yes)
11 msnt.out     -file for transformed data

```

Figure 16: Parameter file for the msnt program.

Parameters for the FORTRAN coded standalone executable msnt\_b (MSNT back-transform) are displayed in Figure 15 and described below:

- **tabfl**: file with the forward MSNT transform data file.
- **nvar**: number of variables to be back-transformed
- **icol(i), i=1,...,nvar**: column locations in the **tabfl** where the original values of the variables are located.
- **icolt(i), i=1,...,nvar**: column locations in the **tabfl** where the transformed values of the variables are located.
- **nclose**: number of nearest mapped observations that should be used for interpolating the back-transformation.
- **datafl**: file with the simulated values that must be back-transformed
- **icold(i), i=1,...,nvar**: column locations in the **datafl** where the simulated values of the variables are located.
- **outfl**: output file containing the back-transformed simulated values.

```

1      MSNT Back Transformation
2      *****
3
4  START OF PARAMETERS:
5  msnt.trn     -transformation data file
6  2            -number of variables
7  1 2          -column numbers: original
8  3 4          -column numbers: transformed
9  2            -number of close values to consider
10 sgsim.out    -file with values to back transform
11 1 2          -column numbers for normal values
12 msnt_b.out   -file for back transformed values

```

Figure 17: Parameter file for the msnt\_b program.